RSC Advances

Cite this: *RSC Advances*, 2012, **2**, 10624–10631

www.rsc.org/advances

PAPER

Preparation of endohedral fullerene containing lithium ($Li@C_{60}$) and isolation as pure hexafluorophosphate salt ($[Li^+@C_{60}][PF_6^-]$)†

Hiroshi Okada,[ab] Takashi Komuro,[a] Takeshi Sakai,[cd] Yutaka Matsuo,[b] Yoshihiro Ono,[e] Kenji Omote,[e] Kuniyoshi Yokoo,[e] Kazuhiko Kawachi,[f] Yasuhiko Kasama,[f] Shoichi Ono,[f] Rikizo Hatakeyama,[g] Toshiro Kaneko[g] and Hiromi Tobita*[a]

Received 21st June 2012, Accepted 10th September 2012
DOI: 10.1039/c2ra21244g

A synthetic protocol for endohedral fullerene containing lithium ($Li@C_{60}$), as well as the synthesis, characterization, and properties of its chemically oxidized derivative $[Li^+@C_{60}][PF_6^-]$ are reported in full. Simultaneous deposition of Li plasma and C_{60} produces a mixture containing $Li@C_{60}$ and C_{60}. Strong intermolecular attraction between $Li@C_{60}$ and C_{60} has prevented their separation, but this obstacle was surmounted by selective chemical oxidation of $Li@C_{60}$, which led to the isolation of a substantial amount of pure $[Li^+@C_{60}][PF_6^-]$. For this purpose, an HPLC technique using an electrolyte in the mobile phase was effective in purifying the ionic metallofullerene. $[Li^+@C_{60}][PF_6^-]$ was stable in air and, compared with $[Li^+@C_{60}][SbCl_6^-]$, was more stable to moisture and various chemicals. $[Li^+@C_{60}][PF_6^-]$ holds promise for practical applications. The spectroscopic data (MS, ^7Li and ^{13}C NMR, UV-vis, and IR) and electrochemical data for $[Li^+@C_{60}][PF_6^-]$ are disclosed. In addition, the high electron affinity of $[Li^+@C_{60}][PF_6^-]$ is discussed.

Introduction

Endohedral fullerene containing lithium ($Li@C_{60}$) is an emerging carbon nanomaterial. The crystal structure of $Li@C_{60}$ has recently been investigated by X-ray diffraction analysis,[1] and its electrochemical properties have been elucidated.[2] $Li@C_{60}$ has features not typically found in endohedral metallofullerenes, whose cages are generally higher fullerenes[3,4] because the inner cavity of the C_{60} cage is too small to easily accommodate lanthanide and transition metal atoms. A lithium atom, however, fits within the C_{60} cage. C_{60} is the most common fullerene and exhibits many fundamental fullerene properties; accordingly, $Li@C_{60}$ is an important type of endohedral metallofullerene.

Smalley and co-workers have observed molecular ion peaks of stable $La@C_{82}$ and of $La@C_{60}$ in the mass spectrum of a sublimed film.[5] Several attempts have been made to prepare endohedral metallo[60]fullerene containing alkaline earth and rare earth metal atoms.[6] Campbell *et al.* have investigated the preparation of alkaline metal-encapsulating C_{60} by low-energy ion bombardment of fullerene films.[7] Except for the preparation of nonmetallic endohedral C_{60}s such as $H_2@C_{60}$[8] and $Ar@C_{60}$,[9] however, the isolation of structurally well-defined endohedral C_{60} was not achieved until our preparation of $Li@C_{60}$.[1]

In that work, we focused primarily on the structure of $Li@C_{60}$ salts. In the present report, we present the full details of the synthesis and characterization of $[Li^+@C_{60}][PF_6^-]$, where the widely used PF_6^- counteranion enables ease of handling. We also report the full details of the preparation of $Li@C_{60}$, which is the precursor to $[Li^+@C_{60}][PF_6^-]$. The synthetic details presented here will facilitate research into endohedral fullerenes and open up new areas of exploration in carbon-based materials science.

Experimental section

General procedure

All solvents, including dehydrated ones, were purchased and used without further purification unless otherwise noted. *o*-Dichlorobenzene for electrochemical measurements was distilled from CaH_2. Tris(4-bromophenyl)ammoniumyl hexachloroantimonate $[(4\text{-}BrC_6H_4)_3NSbCl_6]$ was purchased from Aldrich. All filtrations were performed through a polytetrafluoroethylene-membrane filter (pore size 0.2 μm). All electrochemical measurements were performed in *o*-dichlorobenzene with 50 mM

[a]*Department of Chemistry, Graduate School of Science, Tohoku University, Aoba-ku, Sendai 980-8578, Japan. E-mail: tobita@m.tohoku.ac.jp; Fax: +81 22 795 6539; Tel: +81 22 795 6543*
[b]*Department of Chemistry, School of Science, The University of Tokyo, Bunkyo-ku, Tokyo 113-0033, Japan*
[c]*New Industry Creation Hatchery Center, Tohoku University, Sendai 980-8579, Japan*
[d]*Foundation for Advancement of International Science, Tsukuba 305-0062, Japan*
[e]*Ideal Star Inc. Aoba-ku, Sendai 989-3204, Japan*
[f]*Idea International Corporation, Aoba-ku, Sendai 980-8579, Japan*
[g]*Department of Electronic Engineering, Graduate School of Engineering, Tohoku University, Aoba-ku, Sendai 980-8578, Japan*
† Electronic Supplementary Information (ESI) available: mass spectra of black solid **B**, DLS of black solid **B** and C_{60}, and mass and NMR spectra of $[Li^+@C_{60}][PF_6^-]$. See DOI: 10.1039/c2ra21244g

tetra-*n*-butylammonium hexafluorophosphate ($TBAPF_6$, Wako) as the supporting electrolyte. Cyclic voltammograms (CVs) and differential pulse voltammograms (DPVs) were recorded on a BAS-100B/W with a three-electrode configuration (working electrode, platinum disk of 1.6 mm diameter; counter electrode, Pt wire; reference electrode, 0.01 M $AgNO_3$/Ag and 0.1 M tetra-*n*-butylammonium perchlorate in acetonitrile). The CVs were measured at a scan rate of 100 mV s^{-1}. The DPVs were recorded with pulse amplitude 50 mV; pulse width 50 ms; pulse period 200 ms; and scan rate 20 mV s^{-1}. After the measurements of CV and DPV, ferrocene (Fc) was added to the solution and DPV was measured once again to determine the redox potential values *vs.* Fc^+/Fc. NMR spectra were recorded on a Bruker AVANCE-300 spectrometer (117 MHz for ^{7}Li NMR) and a Bruker AVANCE-600 (151 MHz for ^{13}C NMR) spectrometer. A ^{7}Li NMR spectrum was referred to $LiCl/D_2O$ as the external reference. UV-vis spectra were measured on a Shimadzu MultiSpec-1500 spectrophotometer. IR spectra were recorded on a Horiba FT-730 spectrophotometer. Laser desorption ionization time-of-flight mass spectra (LDI-TOF-MS) were measured on a Shimadzu AXIMA CFR plus. Dynamic light scattering was performed on a Malvern Zetasizer Nano. Elemental analysis was carried out on a J-SCIENCE LAB Micro Corder JM10 for C and H contents. The content of Li was determined by inductively coupled plasma optical emission spectrometry (ICP-OES, Jarrell-Ash IRIS-AP) after the sample treatment by a wet digestion method with HNO_3/H_2SO_4.

Synthesis of Li@C_{60} by irradiation of Li ions to C_{60}

To synthesize Li@C_{60}, we have developed an efficient process by modifying the previously reported methodology for production of K-C_{60} plasma.[10] The apparatus for Li@C_{60} production is schematically shown in Fig. 1. The main chamber in the production apparatus is 100 cm in length and 15 cm in diameter. Energetic Li ions were irradiated to C_{60} in this high-vacuum chamber (1×10^{-5}–1×10^{-4} Pa). Li ions were produced by the contact ionization of Li atoms on a hot rhenium plate of 10 cm in diameter heated up to around 2500 °C by electron bombardment from a tungsten filament. The Li plasma was transported along a magnetic field with the intensity of 500 G to the inclined SUS substrate of 10 cm in diameter and Li ions in the plasma were accelerated within a plasma sheath just in front of the substrate, on which a negative potential of −30 V was applied. C_{60} was simultaneously supplied with Li ions onto the substrate from the fullerene oven at 520–600 °C. The apparatus operated at a Li ion beam current of 10 mA and at a deposition rate of C_{60} of 500 mg h^{-1}. Under growth conditions, the ion to fullerene molar ratio was roughly 0.5. About 1 g of black deposit (**A**) was routinely obtained by one operation for 2 h.

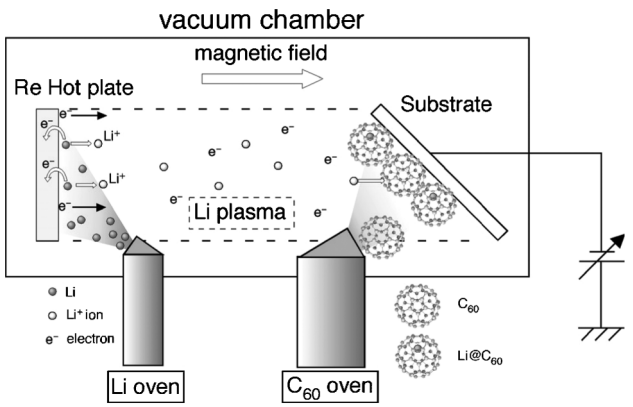

Fig. 1 Schematic diagram of the production apparatus for endohedral fullerene containing Li. Li^+ ions produced by contact ionization are supplied together with C_{60} molecules onto a metal substrate. The ions are accelerated by negative potential applied to the substrate, and a suitable amount of C_{60} is generated from a heated copper oven by sublimation.

Extraction and concentration of Li@C_{60} with 1-chloronaphthalene

The deposit **A** (*ca.* 1 g) was collected and dispersed into hydrochloric acid (0.05 M, 15 mL) overnight to oxidize lithium atoms *outside* the C_{60} cages to Li ions. The suspension was filtered and the black solid on the filter was washed with water to remove water-soluble substances such as Li^+ salts. The resulting black solid was dried at 100 °C under vacuum. Several solvents (toluene, carbon disulfide, *o*-dichlorobenzene, pyridine, acetonitrile, and 1-chloronaphthalene) were examined to extract Li@C_{60} from the HCl-washed black solid. The extraction efficiency was estimated by the Li@C_{60} peak intensity (m/z = 727) of the LDI-TOF mass spectra of extracted solutions, and 1-chloronaphthalene was found to be the most efficient extracting solvent among them. Thus, after the above-mentioned HCl-washing procedure was carried out for several samples, the combined black solid (6.00 g) was added into 1-chloronaphthalene (120 mL) and stirred overnight. The brown suspension was filtered, and to the filtrate was added toluene (600 mL) to precipitate out a Li@C_{60} rich component. After 21 h, the mixture was filtered. The precipitate on the filter was washed with hexane and dried under reduced pressure to afford a brown solid **B** (290 mg). The Li content of **B** determined by ICP-OES was 0.059%, which corresponds to the Li@C_{60} purity of *ca.* 6 wt%. LDI-TOF mass spectra of the solid **B** are depicted in Fig. S1, see ESI.† Dynamic light scattering of 1-chloronaphthalene solutions of the solid **B** and C_{60} is shown in Fig. S2, see ESI.†

Chemical oxidation of Li@C_{60}

Deposit **A** on the substrate was transferred into an argon-filled glove box immediately after the synthetic procedure, and used for the next oxidation process. The deposit **A** (5.59 g) and tris(4-bromophenyl)ammoniumyl hexachloroantimonate (8.39 g, 10.3 mmol) were placed in a 500 mL flask, and dehydrated *o*-dichlorobenzene (280 mL) and acetonitrile (140 mL) were added into it. A dark blue suspension in the flask was stirred at room temperature under an argon atmosphere for 24 h. Then the flask was brought out of the glove box, and after most of acetonitrile was removed from the resulting dark purplish-brown suspension under reduced pressure, toluene (600 mL) and hexane (300 mL) were added to it. The mixture was allowed to stand for 1 h to produce a brown fine-grained precipitate, which was filtered and washed repeatedly with acetonitrile (three times, 750 mL in total) and toluene (300 mL). The $[Li@C_{60}]^+$ salt was extracted from the brown residue by *o*-dichlorobenzene–acetonitrile (v/v = 1 : 1).

Purification of a product $[Li^+@C_{60}][SbCl_6^-]$

The extract of the $[Li@C_{60}]^+$ salt was evaporated under reduced pressure to remove most of the acetonitrile in the solution. The brown solids precipitated out. The suspension was kept at 5 °C for 2 days, and then filtered to collect brown solids that contained $[Li^+@C_{60}][SbCl_6^-]$ as a main component. Typically, *ca.* 20 mg of the brown solid was obtained from 5.7 g of the deposit **A**. The purity of the brown solids was not adequate for elemental analysis at this stage. Repeated recrystallization eventually gave pure crystals of $[Li^+@C_{60}][SbCl_6^-]$, but the recovery rate was 10% at most. $[Li^+@C_{60}][SbCl_6^-]$ was identified by comparing the spectroscopic and analytical data with the literature values in ref. 1*a*.

Purification of the product by HPLC to isolate $[Li^+@C_{60}][PF_6^-]$

The above-mentioned oxidation and extraction processes were repeated three times. The combined extract (*ca.* 480 mL) was pretreated by a cation-exchange SPE (solid-phase-extraction) cartridge (sulfo-group-substituted silica gel, 10 g, inertSep-SCX, GL science) before HPLC purification to remove the impurities that damage the HPLC column. Thus, the extract was passed through an SPE cartridge in which the cation had been previously changed to tetra-*n*-butylammonium to make all $[Li@C_{60}]^+$ ions in the extract absorb in the stationary phase. The electrolyte solution (50 mM $TBAPF_6$, *o*-dichlorobenzene–acetonitrile, v/v = 1 : 2) was then passed through the $Li@C_{60}^+$-adsorbed cartridge to give a purple eluate, which was injected into a 5NPE column (10 mm i.d. × 250 mm; Cosmosil, Nacalai Tesque Inc.) on HPLC. *o*-Dichlorobenzene–acetonitrile (v/v = 1 : 2) containing 50 mM $TBAPF_6$ was used as the eluent, and a peak corresponding to the $[Li@C_{60}]^+$ ion was collected. Acetonitrile was removed from the fraction under reduced pressure, and hexane was added into the residual solution to precipitate all of the ionic materials. The precipitate, including a large amount of $TBAPF_6$, was washed with acetonitrile repeatedly (40 mL in total) to afford $[Li^+@C_{60}][PF_6^-]$ as a dark brown solid. From 16.7 g of deposit **A**, 29.0 mg of almost pure $[Li^+@C_{60}][PF_6^-]$ was obtained. The purity of $[Li^+@C_{60}][PF_6^-]$ was confirmed not only by the LDI-TOF mass spectra in negative mode but also by the ^{13}C and ^{7}Li NMR spectra. The Li content of the $[Li^+@C_{60}][PF_6^-]$ sample determined by ICP-OES (0.66 wt%) corresponds to *ca.* 85% purity of $[Li^+@C_{60}][PF_6^-]$. To get a purer sample suitable for elemental analysis, it was re-extracted as follows. The solid was dissolved in chlorobenzene–acetonitrile (v/v = 1 : 1) and filtered. The filtrate was evaporated under reduced pressure. The resulting brown solid was washed with small amounts of *o*-dichlorobenzene, toluene, and hexane, and was dried under reduced pressure. $^{13}C\{^1H\}$ NMR (151 MHz, *o*-dichlorobenzene-d_4–acetonitrile-d_3 = 1 : 1): δ 142.68. ^{7}Li NMR (117 MHz, *o*-dichlorobenzene-d_4–acetonitrile-d_3 = 1 : 1, LiCl in D_2O as external standard): δ −10.5. Anal. Calcd. for $C_{60}F_6LiP$: C, 82.59; H, 0.00; Li, 0.80. Found: C, 82.269; H, 0.595; Li, 0.756. LDI-TOF MS: 727 (M^+). IR spectra (KBr): 1419, 1181, 578, 530 ($Li^+@C_{60}$), 837, 559 (PF_6^-) cm^{-1}. C_{60}: $^{13}C\{^1H\}$ NMR (151 MHz, *o*-dichlorobenzene-d_4–acetonitrile-d_3 = 1 : 1): δ 143.31. IR spectra (KBr): 1428, 1182, 576, 526 cm^{-1}.

Results and discussion

Synthesis and attempted purification of neutral $Li@C_{60}$

As a method for the mass production of $Li@C_{60}$, an ion beam technique based on ion implantation was used.[7,11] A high-current beam of Li^+ ions with low energy and a beam of neutral C_{60} molecules were simultaneously supplied onto a metal substrate. The contact ionization method is useful for producing endohedral alkali-fullerenes, because high-density alkali plasma is produced with sufficiently low ion energy dispersion, which is necessary in order to avoid fullerene fragmentation and polymerization.

A black deposit (**A**) that accumulated on the substrate was collected and analyzed by laser desorption–ionization time-of-flight mass spectrometry (LDI-TOF MS; positive mode), which showed a strong peak of m/z = 727, which is attributable to the parent ion $[Li@C_{60}]^+$.[1a]

From deposit **A**, we tried to extract $Li@C_{60}$ with several different solvents, and found that 1-chloronaphthalene was an effective solvent for this purpose. Thus, extraction with 1-chloronaphthalene and re-precipitation with toluene afforded a $Li@C_{60}$-enriched brown solid (**B**), of which the positive-mode LDI-TOF MS showed an increased intensity of the $Li@C_{60}$ molecular ion peak relative to that of the C_{60} peak. Upon repeated extraction and re-precipitation, the relative intensity increased to about 5–10 (Fig. S1a, see ESI†), but plateaued. Interestingly, even at this level of enrichment, the negative-mode LDI-TOF MS did not show any recognizable peak at m/z = 727 (Fig. S1b, see ESI†). This is probably because an extra electron for anion formation is less readily added to $Li@C_{60}$ (which already has a negatively charged fullerene cage), as compared with a C_{60} molecule. The lithium content of **B** was determined to be 0.059 wt%, which corresponds to a $Li@C_{60}$ abundance of only 6 wt% (the theoretical Li content of pure $Li@C_{60}$ is 0.95 wt%). After a few dozen experiments, we found that the lithium content of **B** consistently fell within the range 0.05–0.08 wt% (5–8 wt% $Li@C_{60}$) (Scheme 1).

These results suggest the formation of clusters composed of a $Li@C_{60}$ molecule and more than 10 C_{60} molecules. Particle size analysis of **B** by dynamic light scattering showed the diameter to be 3–7 nm (Fig. S2a, see ESI†), which supports this hypothesis. The nature of the strong intermolecular interaction between $Li@C_{60}$ and C_{60} has not yet been clarified, but it might be attributable either to a charge transfer interaction between the SOMO of the negatively charged C_{60} cage of $Li@C_{60}$ and the LUMO of C_{60} molecules, or to the formation of covalent bonds

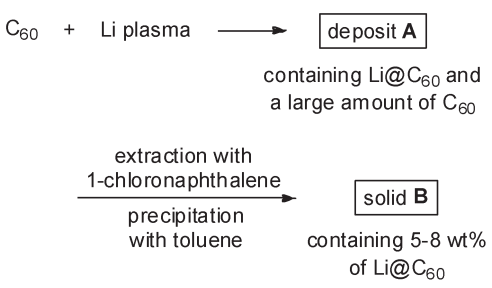

Scheme 1 Synthetic scheme to obtain deposit **A** and solid **B**.

between them *via* a further reaction as suggested by Gromov *et al.*[7b]

Chemical oxidation of Li@C_{60} giving [Li^+@C_{60}] salts

To suppress this interaction between Li@C_{60} and C_{60} molecules, we examined the chemical oxidation of the product. One-electron oxidation occurs selectively at the more electropositive Li@C_{60} to give [Li^+@C_{60}], in which it is considered that the positive charge is concentrated mostly on lithium to form a Li cation and the C_{60} cage behaves like a neutral C_{60} molecule. We expected that this change would break up the cluster into isolable Li@C_{60} and C_{60} units. A few examples of chemical oxidation and separation of endohedral metallofullerenes have been reported for M@C_{82} (M = Y, La, Ce),[12] Sc_3N@C_{80},[13] and M@C_{2n} (M = Gd, Tm, $2n$ = 60, 70, and $\geqslant$72).[14]

The mixture of Li@C_{60} and C_{60}, deposit **A**, was oxidized to give the monomeric Li@C_{60} cation, which was isolated as an $SbCl_6^-$ salt, [Li^+@C_{60}][$SbCl_6^-$], as a brown solid (Scheme 2). A single crystal of [Li^+@C_{60}][$SbCl_6^-$] was obtained by recrystallization, and we have recently reported the X-ray crystal structure analysis of [Li^+@C_{60}][$SbCl_6^-$],[1a] which was the first crystal structure determination of a metal-encapsulating C_{60}.

We quickly discovered that, in repeated recrystallizations for purification, [Li^+@C_{60}][$SbCl_6^-$] was slightly unstable, especially to moisture (a possible decomposition pathway is hydrolysis of the counter anion), which probably caused the poor recovery rate from recrystallization. We therefore examined the purification of [Li^+@C_{60}][$SbCl_6^-$] by HPLC. Eventually, we found that a COSMOSIL 5NPE packed column (a nitrophenylethyl-group-bonded silica gel column) was effective for separating the [Li^+@C_{60}] ion. The addition of the electrolyte tetra-*n*-butylammonium hexafluorophosphate ($TBAPF_6$) into the mobile phase was critical. Fig. 2 shows the HPLC chromatograms of purified [Li^+@C_{60}][$SbCl_6^-$] with and without $TBAPF_6$ in the mobile phase. No peak was observed in the absence of an electrolyte (Fig. 2a), while a clear peak for the [Li^+@C_{60}] ion was observed in the presence of the electrolyte (Fig. 2b). After optimizing the mobile phase conditions, we succeeded in separating and completely purifying the [Li^+@C_{60}] ion from the crude mixture of oxidation products by this HPLC technique. The chromatogram of crude extract containing [Li^+@C_{60}] has multiple peaks (Fig. 3a), whereas the chromatogram of the pure [Li^+@C_{60}][PF_6^-] isolated by HPLC has only a single peak (Fig. 3b). During elution, the counteranion was completely changed from $SbCl_6^-$ to PF_6^-, and pure [Li^+@C_{60}][PF_6^-] was isolated from the eluate. This chromatographic method is quite efficient, and we were able to steadily purify a substantial amount of [Li^+@C_{60}][PF_6^-] in a short time. Importantly, the hexafluorophosphate salt [Li^+@C_{60}][PF_6^-] is stable in air and

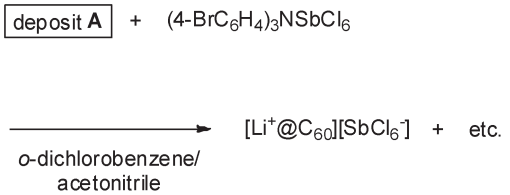

Scheme 2 Synthetic scheme to obtain the $SbCl_6$ salt [Li^+@C_{60}][$SbCl_6^-$].

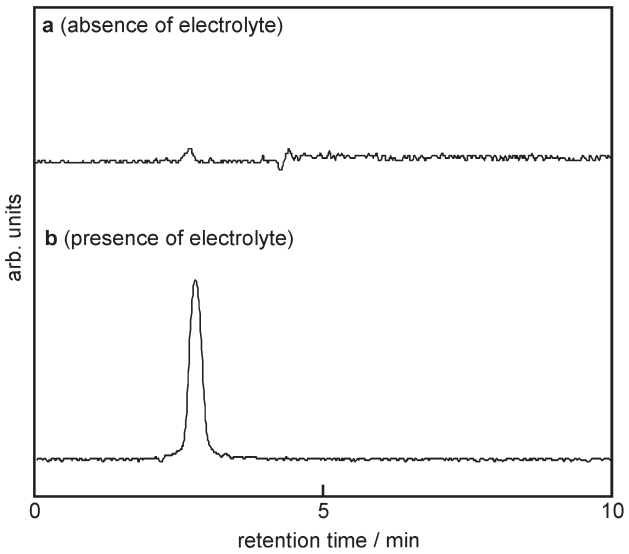

Fig. 2 HPLC chromatograms of [Li^+@C_{60}][$SbCl_6^-$] when the mobile phase (*o*-dichlorobenzene–acetonitrile, v/v = 1 : 1) contained (a) no electrolyte and (b) 20 mM tetra-n-butylammonium hexafluorophosphate. Column: 5NPE (4.6 mm i.d. × 250 mm). Flow rate: 1.5 mL min^{-1}.

significantly more stable to moisture than the hexachloroantimonate salt [Li^+@C_{60}][$SbCl_6^-$], and thus should be more suitable for physical and chemical investigations.

Spectroscopic data for [Li^+@C_{60}][PF_6^-]

The LDI-TOF mass spectra of [Li^+@C_{60}][PF_6^-] are shown in Fig. 4 (see also Fig. S3, see ESI†). The positive-mode spectrum and the negative-mode spectrum show a strong peak at m/z = 727, which is assigned to Li^+@C_{60}. Considering that C_{60} is a better electron acceptor than Li^+@C_{60}, the absence of the C_{60} molecular ion peak (m/z = 720) in the negative-mode spectrum of

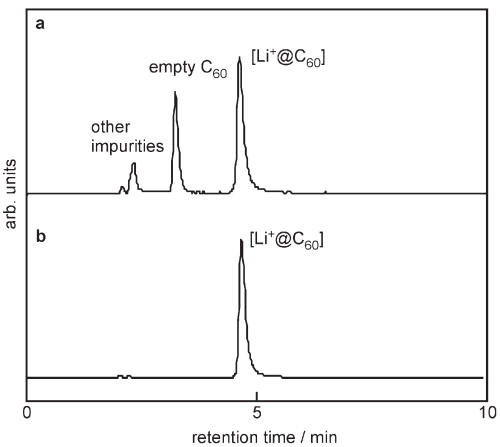

Fig. 3 Comparison of the chromatographs from HPLC using electrolyte in the mobile phase: (a) crude *o*-dichlorobenzene–acetonitrile extract containing the [Li^+@C_{60}], and (b) pure [Li^+@C_{60}][PF_6^-]. Eluent: *o*-dichlorobenzene–acetonitrile (v/v = 1 : 2) with 50 mM tetra-*n*-butylammonium hexafluorophosphate. Column: 5NPE (4.6 mm i.d. × 250 mm). Flow rate: 1.5 mL min^{-1}.

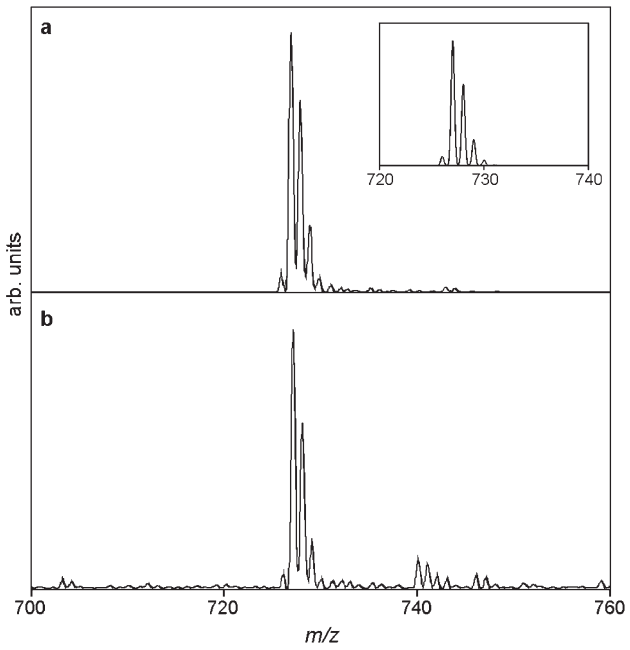

Fig. 4 LDI-TOF-MS of $[Li^+@C_{60}][PF_6^-]$ in the range m/z = 700–760: (a) reflectron positive mode and (b) reflectron negative mode. Inset: isotope distribution pattern of $C_{60}Li$.

$[Li^+@C_{60}][PF_6^-]$ strongly suggests that the C_{60} was completely removed.

The ^7Li and ^{13}C NMR signals of $[Li^+@C_{60}][PF_6^-]$ are sharp at room temperature (Fig. 5), clearly indicating the material's diamagnetic nature. The ^7Li NMR spectrum of $[Li^+@C_{60}][PF_6^-]$ (Fig. 5a, see also Fig. S4, see ESI†) shows a peak at high field (δ −10.5 ppm relative to LiCl in D_2O). Bühl *et al.* have predicted by *ab initio* calculation that the ^7Li chemical shift of $[Li^+@C_{60}]$ is around −15 ppm relative to that of $[Li(OH_2)_4]^+$.[15] For an atom or molecule encapsulated in a C_{60} cage, a similar upfield shift has been reported relative to the free species: $H_2@C_{60}$ (δ −1.44 ppm, shifted 5.98 ppm upfield relative to free H_2) in ^1H NMR,[7] $He@C_{60}$ (δ −6.4 ppm, relative to free ^3He) in ^3He NMR,[16] and $Xe@C_{60}$ (δ −8.89 ppm, relative to free ^{129}Xe) in ^{129}Xe NMR.[17] These upfield shifts can be explained by the shielding effect of the π-conjugated system of C_{60}.[18] The ^{13}C NMR spectrum of $[Li^+@C_{60}][PF_6^-]$ (Fig. 5b, see also Fig. S5, see ESI†) in *o*-dichlorobenzene-d_4–acetonitrile-d_3 (v/v = 1 : 1) exhibits a single peak at 142.68 ppm. In comparison with the chemical shift of C_{60} in the same solvent (143.31 ppm, shown in Fig. 5c), a small but significant upfield shift (0.63 ppm) was observed. This suggests that, in a salt of the $[Li^+@C_{60}]$ ion, the positive charge is located on the lithium atom exclusively and the C_{60} cage is neutral. The inclusion of a lithium cation causes an upfield shift of the ^{13}C NMR signal of the C_{60} cage, while it has been reported that the inclusion of noble gases or dihydrogen causes a downfield shift: 0.17 ppm for $Ar@C_{60}$,[8] 0.39 ppm for $Kr@C_{60}$,[19] 0.96 ppm for $Xe@C_{60}$,[17] and 0.078 ppm for $H_2@C_{60}$.[7] Moreover, the observation of only one signal in the ^{13}C NMR spectrum clearly shows that in solution, the lithium cation in $[Li^+@C_{60}][PF_6^-]$ is either located at the center of the I_h-symmetric C_{60} cage or displaced from the center, but moves faster than the NMR timescale within the cage.

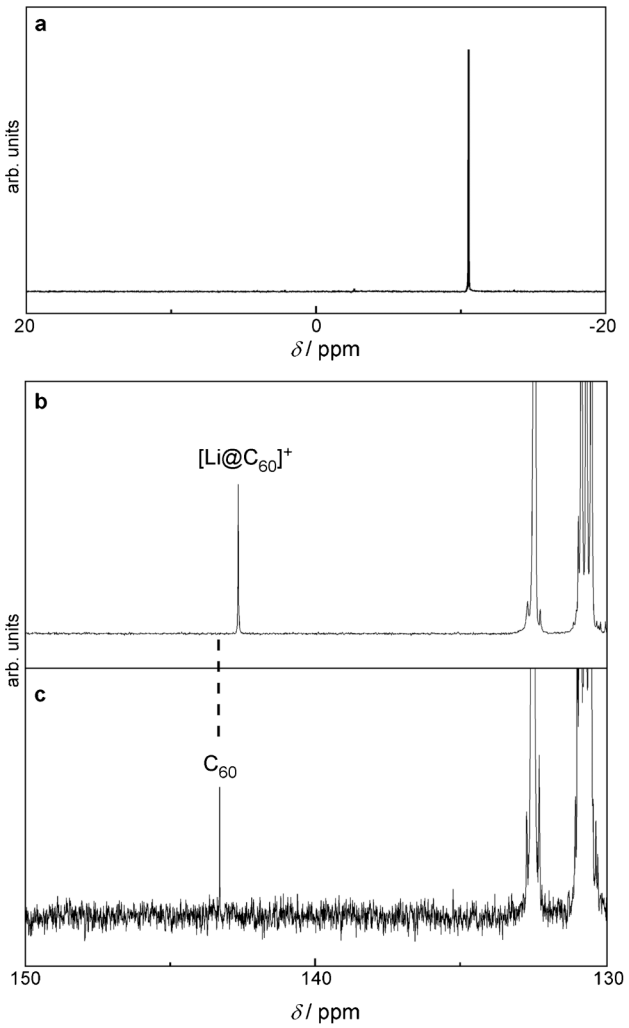

Fig. 5 NMR spectra of $[Li^+@C_{60}][PF_6^-]$ and C_{60}: (a) ^7Li NMR of $[Li^+@C_{60}][PF_6^-]$, (b) ^{13}C NMR of $[Li^+@C_{60}][PF_6^-]$, and (c) ^{13}C NMR of C_{60}. (117 MHz for ^7Li NMR and 151 MHz for ^{13}C NMR; *o*-dichlorobenzene-d_4–acetonitrile-d_3 = 1 : 1).

The UV-vis spectrum of $[Li^+@C_{60}][PF_6^-]$ at room temperature is shown in Fig. 6 together with that of C_{60}. As in the case of the $SbCl_6^-$ salt, the features and wavelengths of the absorption maxima of the spectrum of $[Li^+@C_{60}][PF_6^-]$ are similar to those of C_{60}. Thus, the dipole-allowed transition of $[Li^+@C_{60}][PF_6^-]$ appears at λ_{max} 335 nm (ε = 6.0 × 10^4 M^{-1} cm^{-1}), with significant broadening of the band compared with that of C_{60} [λ_{max} 334 nm (ε = 5.2 × 10^4 M^{-1} cm^{-1})]. The dipole-forbidden transitions are observed at λ_{max} 544 nm (ε = 1.3 × 10^3 M^{-1} cm^{-1}) and 599 nm (ε = 1.0 × 10^3 M^{-1} cm^{-1}), with larger extinction coefficients compared with those of C_{60} [λ_{max} 539 nm (ε = 8.1 × 10^2 M^{-1} cm^{-1}) and 598 nm (ε = 7.0 × 10^2 M^{-1} cm^{-1})]. These observations indicate that the interaction between the encapsulated lithium cation and the C_{60} cage barely alters the intervals between the energy levels of the frontier orbitals. In contrast, the absolute energy levels of the frontier orbitals of $[Li^+@C_{60}]$ are substantially different from those of C_{60}, which will be discussed in detail in the section on electrochemical properties.

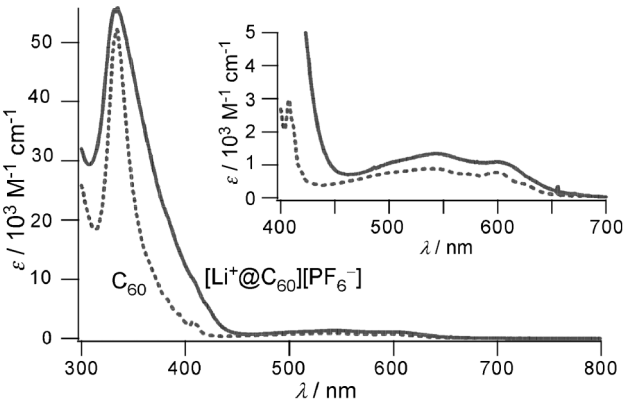

Fig. 6 UV-vis spectra of (a) $[Li^+@C_{60}][PF_6^-]$ (solid line) and (b) C_{60} (dotted line) in *o*-dichlorobenzene.

The IR spectrum of $[Li^+@C_{60}][PF_6^-]$ at room temperature is shown in Fig. 7, together with that of C_{60}. Four peaks assignable to the $[Li^+@C_{60}]$ ion are observed at 1419, 1181, 578, and 530 cm^{-1}, excluding the peaks for the PF_6^- ion at 837 and 559 cm^{-1}.[20] The spectroscopic features of the $[Li^+@C_{60}]$ ion are almost identical to those of C_{60} (1428, 1182, 576, and 526 cm^{-1}), but the peaks are slightly shifted. The largest shift (9 cm^{-1}), which was observed for the highest wavenumber peak, was toward low energy and may be attributable to the interaction of the π electrons with the encapsulated lithium cation. Importantly, only four distinct IR peaks are observed for the $[Li^+@C_{60}]$ part of $[Li^+@C_{60}][PF_6^-]$. We previously demonstrated by structural analysis using synchrotron radiation X-ray diffraction that, in the solid state of $[Li^+@C_{60}][SbCl_6^-]$, the encapsulated lithium cation takes a specific off-center position near a six-membered ring inside the C_{60} cage.[1] Since the IR spectrum of $[Li^+@C_{60}][PF_6^-]$ is almost identical to that of $[Li^+@C_{60}][SbCl_6^-]$, except for the peaks for the counteranion, the lithium cation in the C_{60} cage of $[Li^+@C_{60}][PF_6^-]$ is also presumed to be located at a similarly off-center position. However, the symmetry of this structure, C_{3v}, is lower than that of C_{60}, I_h. Therefore, if a lithium cation inside a C_{60} cage is fixed at the off-center position, more than four IR peaks should appear for the $[Li^+@C_{60}]$ part. There are at least two possible explanations for why these peaks were not observed. Firstly, the lithium cation inside the C_{60} cage hops among the twenty stable positions faster than the vibrational timescale. There have been some reports on the coalescence of IR bands in very fast

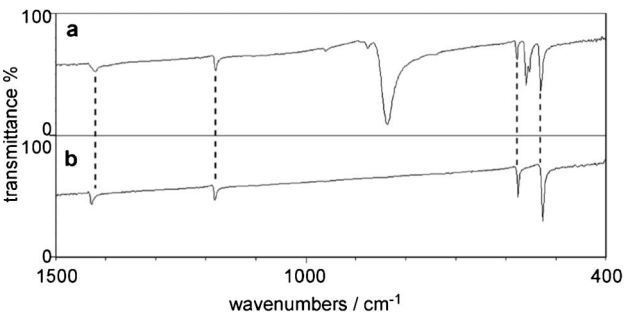

Fig. 7 IR spectra of (a) $[Li^+@C_{60}][PF_6^-]$ and (b) C_{60} (KBr pellet).

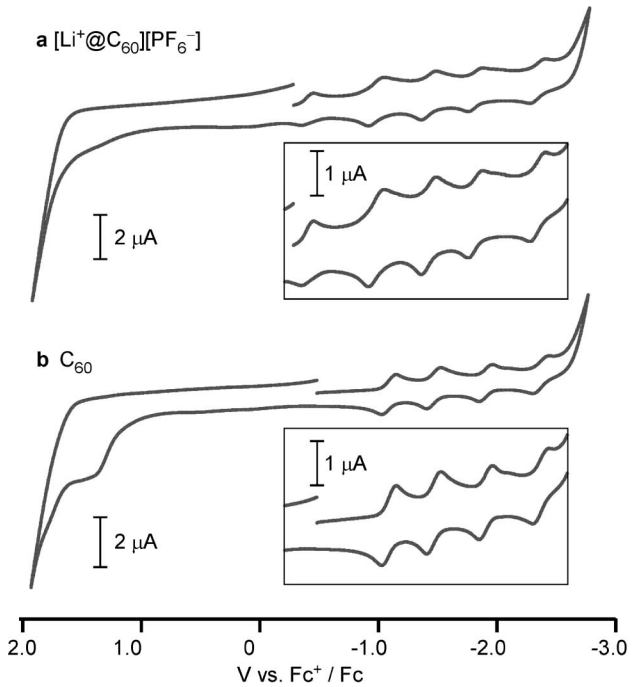

Fig. 8 CVs of (a) $[Li^+@C_{60}][PF_6]$ and (b) C_{60} in *o*-dichlorobenzene containing 50 mM tetra-*n*-butylammonium hexafluorophosphate as the supporting electrolyte. Working electrode: Pt; counter electrode: Pt; scan rate: 100 mV s^{-1}. Inset: expanded voltammograms in negative potential region.

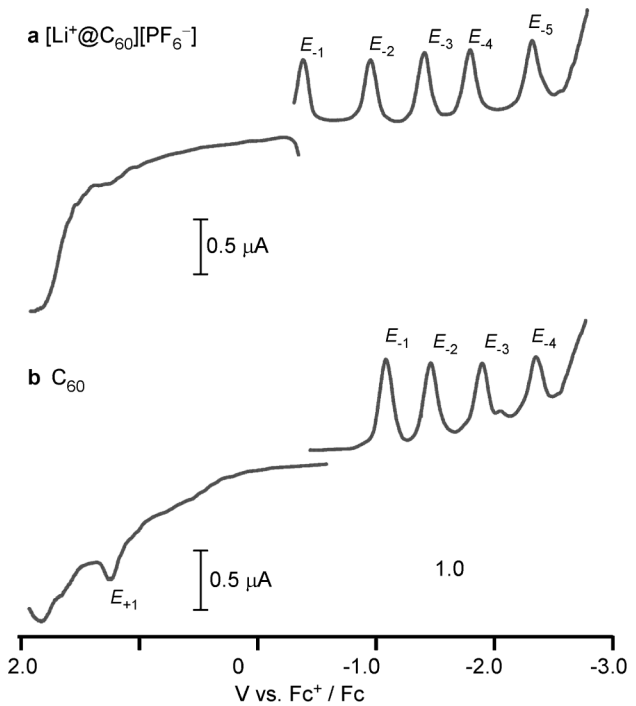

Fig. 9 DPVs of (a) $[Li^+@C_{60}][PF_6^-]$ and (b) C_{60} in *o*-dichlorobenzene containing 50 mM tetra-*n*-butylammonium hexafluorophosphate as the supporting electrolyte. Working electrode: Pt; counter electrode: Pt; pulse amplitude: 50 mV; pulse width: 50 ms; pulse period: 200 ms; scan rate: 20 mV s^{-1}.

Table 1 Peak potentials[a] of $[Li^+@C_{60}][PF_6^-]$ and C_{60}, measured by differential pulse voltammetry[b]

	E_{+1}	E_{-1}	E_{-2}	E_{-3}	E_{-4}	E_{-5}
	V vs. Fc^+/Fc					
$[Li^+@C_{60}][PF_6^-]$	—	−0.38	−0.95	−1.41	−1.79	−2.32
C_{60}	+1.26	−1.08	−1.46	−1.90	−2.35	—

[a] *V vs.* Fc^+/Fc. [b] In *o*-dichlorobenzene with 50 mM tetra-*n*-butyl-ammonium hexafluorophosphate as the supporting electrolyte; working electrode: Pt, counter electrode: Pt.

chemical exchange processes, such as the intramolecular electron transfer in pyrazine-bridged trinuclear ruthenium dimers[21] and the exchange of three carbonyl ligands in (η^4-diene)$Fe(CO)_3$ complexes.[22] Secondly, even if the lithium cation is located at the off-center position, the symmetry of the C_{60} cage will not be lowered to a great extent; thus most of the IR active bands of the C_{60} cage with C_{3v} symmetry, except for those corresponding to the four IR active bands of the I_h-symmetric C_{60}, will be very weak and virtually unobservable. At present, we have no experimental results that can rule out either possible explanation.

Electrochemical properties of $[Li^+@C_{60}][PF_6^-]$

We investigated the electrochemical properties of $[Li^+@C_{60}][PF_6^-]$ by measuring its cyclic voltammogram (CV) and differential pulse voltammogram (DPV) in the range +2.0 to −2.75 V *vs.* the potential of the ferrocenium (Fc^+)/ferrocene (Fc) redox couple (Fig. 8 and 9). The CVs of $[Li^+@C_{60}][PF_6^-]$ (Fig. 8a) and C_{60} (Fig. 8b) exhibit five and four reversible or quasi-reversible redox waves, respectively, in the range 0 to −2.75 V. In the range +2.0 to 0 V, C_{60} shows an irreversible oxidation wave, whereas $[Li^+@C_{60}][PF_6^-]$ does not show any oxidation wave in this region. The peak potentials *vs.* Fc^+/Fc for $[Li^+@C_{60}][PF_6^-]$ and C_{60} determined by DPVs (Fig. 9) are listed in Table 1. Note that the first reduction of $[Li^+@C_{60}][PF_6^-]$ (E_{-1} = −0.38 V) corresponds to the first reduction of the neutral C_{60} cage to the anion C_{60}^- (E_{-1} = −1.08 V).

The first to fourth reduction potentials (E_{-1} to E_{-4}) of $[Li^+@C_{60}][PF_6^-]$ are shifted to the positive side by 0.70, 0.51, 0.49, and 0.56 V, respectively, in comparison with those of C_{60}. Similarly, E_{+1} of $[Li^+@C_{60}][PF_6^-]$ is also shifted from E_{+1} of C_{60} (E_{+1} = +1.26 V) toward the positive side by a similar magnitude to be driven out of the potential window. This phenomenon clearly indicates that the LUMO and HOMO of $[Li^+@C_{60}][PF_6^-]$ are much lower than those of C_{60}, and therefore $[Li^+@C_{60}][PF_6^-]$ is an even stronger electron acceptor than C_{60}. As mentioned in the section on UV-vis spectra, the energy differences between the frontier orbitals were largely unchanged by encapsulation of Li^+ in the C_{60} cage. This means that both the LUMO and HOMO of $[Li^+@C_{60}][PF_6^-]$ are stabilized to almost the same extent in comparison with those of C_{60}. This stabilization is mainly attributable to the Coulomb interaction between the encapsulated lithium cation and the C_{60} cage.[23] According to the first reduction potential, $[Li^+@C_{60}][PF_6^-]$ should be easily reduced to neutral $Li@C_{60}$. We are now attempting the one-electron reduction of $[Li^+@C_{60}][PF_6^-]$ to prepare a pure form of $Li@C_{60}$.

Conclusions

Preparation of $Li@C_{60}$ by simultaneous deposition of Li plasma and C_{60} followed by chemical oxidation of $Li@C_{60}$ with (4-$BrC_6H_4)_3NSbCl_6$ provided a product mixture containing $[Li^+@C_{60}][SbCl_6^-]$. This salt was successfully purified by a special HPLC technique using a mobile phase composed of *o*-dichlorobenzene and acetonitrile (v/v = 1 : 2) with an added electrolyte ($TBAPF_6$). This procedure resulted in exchange of the counteranion to afford a substantial amount of pure $[Li^+@C_{60}][PF_6^-]$. $[Li^+@C_{60}][SbCl_6^-]$ and $[Li^+@C_{60}][PF_6^-]$ are the first endohedral metallo[60]fullerenes that have been isolated and fully characterized. A solution of $[Li^+@C_{60}][PF_6^-]$ in *o*-dichlorobenzene-d_4–acetonitrile-d_3 (v/v = 1 : 1) showed a ^7Li NMR signal at high field (−10.5 ppm relative to LiCl in D_2O), owing to the shielding effect of the π-system of C_{60}, and a single ^{13}C NMR signal at 142.68 ppm at room temperature, indicating that the Li cation moves faster than the NMR timescale within the C_{60} cage. The IR and UV-vis spectra of $[Li^+@C_{60}][PF_6^-]$ were almost identical to those of C_{60}, indicating that the vibrational structure and energy gap between the frontier orbitals are not altered by encapsulation of Li^+. In sharp contrast, electrochemical studies of $[Li^+@C_{60}][PF_6^-]$ showed a substantial shift of reduction waves to the positive side in relation to those of C_{60}. This stabilization of frontier orbitals is mainly attributed to the Coulomb interaction between the encaged Li cation and the C_{60} cage, and therefore, $[Li^+@C_{60}][PF_6^-]$ is a stronger electron acceptor than C_{60}. The well-characterized $[Li^+@C_{60}]$ salts might be applicable for materials research.[24] Furthermore, the present methodology for preparing and purifying lithium-endohedral C_{60} will provide a new method to access other types of endohedral metallo[60]fullerenes.

Acknowledgements

The authors thank Professor N. Sato and Dr T. Hirata, whose plasma experiments provided valuable information about the efficient synthesis of endohedral alkali-fullerene. We are grateful to Dr Y. Takabayashi for fruitful discussion. We also acknowledge the Technical Division, School of Engineering, and Analytical Center for Giant Molecules, School of Science, in Tohoku University, for spectroscopic and analytical measurements. This work was supported by a Grant-in-Aid for Scientific Research No. 23655046 from the Ministry of Education, Culture, Sports, Science and Technology, Japan, and the Funding Program for Next Generation World-Leading Researchers.

References

1 (*a*) S. Aoyagi, E. Nishibori, H. Sawa, K. Sugimoto, M. Takata, Y. Miyata, R. Kitaura, H. Shinohara, H. Okada, T. Sakai, Y. Ono, K. Kawachi, K. Yokoo, S. Ono, K. Omote, Y. Kasama, S. Ishikawa, T. Komuro and H. Tobita, *Nat. Chem.*, 2010, **2**, 678; (*b*) S. Aoyagi, Y.

Sado, E. Nishibori, H. Sawa, H. Okada, H. Tobita, Y. Kasama, R. Kitaura and H. Shinohara, *Angew. Chem., Int. Ed.*, 2012, **51**, 3377.
2 (*a*) S. Fukuzumi, K. Ohkubo, Y. Kawashima, D. S. Kim, J. S. Park, A. Jana, V. M. Lynch, D. Kim and J. L. Sessler, *J. Am. Chem. Soc.*, 2011, **133**, 15938; (*b*) K. Ohkubo, Y. Kawashima and S. Fukuzumi, *Chem. Commun.*, 2012, **48**, 4314.
3 H. Shinohara, *Rep. Prog. Phys.*, 2000, **63**, 843.
4 *Endofullerenes: A New Family of Carbon Clusters*, ed. T. Akasaka and S. Nagase, Kluwer, Dordrecht, 2002.
5 (*a*) J. R. Heath, S. C. O'Brien, Q. Zhang, Y. Liu, R. F. Curl, H. W. Kroto, F. K. Tittel and R. E. Smalley, *J. Am. Chem. Soc.*, 1985, **107**, 7779; (*b*) Y. Chai, T. Guo, C. Jin, R. E. Haufler, L. P. F. Chibante, J. Fure, L. Wang, J. M. Alford and R. E. Smalley, *J. Phys. Chem.*, 1991, **95**, 7564.
6 (*a*) T. Inoue, Y. Kubozono, S. Kashino, Y. Takabayashi, K. Fujitaka, M. Hida, M. Inoue, T. Kanbara, S. Emura and T. Uruga, *Chem. Phys. Lett.*, 2000, **316**, 381; (*b*) T. Kanbara, Y. Kubozono, Y. Takabayashi, S. Fujiki, S. Iida, Y. Haruyama, S. Kashino, S. Emura and T. Akasaka, *Phys. Rev. B: Condens. Matter*, 2001, **64**, 113403 and references cited therein.
7 (*a*) R. Tellgmann, N. Krawez, S.-H. Lin, I. V. Hertel and E. E. B. Campbell, *Nature*, 1996, **382**, 407; (*b*) A. Gromov, D. Ostrovskii, A. Lassesson, M. Jönsson and E. E. B. Campbell, *J. Phys. Chem. B*, 2003, **107**, 11290; (*c*) V. N. Popok, I. I. Azarko, A. V. Gromov, M. Jönsson, A. Lassesson and E. E. B. Campbell, *Solid State Commun.*, 2005, **133**, 499 and references cited therein.
8 K. Komatsu, M. Murata and Y. Murata, *Science*, 2005, **307**, 238.
9 K. Yakigaya, A. Takeda, Y. Yokoyama, S. Ito, T. Miyazaki, T. Suetsuna, H. Shimotani, T. Kakiuchi, H. Sawa, H. Takagi, K. Kitazawa and N. Dragoe, *New J. Chem.*, 2007, **31**, 973.
10 T. Hirata, R. Hatakeyama, T. Mieno and N. Sato, *J. Vac. Sci. Technol., A*, 1996, **14**, 615.
11 H. Okada, Y. Shibata, K. Yokoo, Y. Mizobuchi, K. Omote and Y. Kasama, *Patent Application Publication, Pub. No.: US 2009/0105386 A1*, 23 April, 2009.
12 (*a*) Y. Maeda, J. Miyashita, T. Hasegawa, T. Wakahara, T. Tsuchiya, L. Feng, Y. Lian, T. Akasaka, K. Kobayashi, S. Nagase, M. Kato, K. Yamamoto and K. M. Kadish, *J. Am. Chem. Soc.*, 2005, **127**, 2143; (*b*) T. Tsuchiya, T. Wakahara, Y. Lian, Y. Maeda, T. Akasaka, T. Kato, N. Mizorogi and S. Nagase, *J. Phys. Chem. B*, 2006, **110**, 22517.
13 B. Elliott, L. Yu and L. Echegoyen, *J. Am. Chem. Soc.*, 2005, **127**, 10885.
14 R. D. Bolskar and J. M. Alford, *Chem. Commun.*, 2003, 1292.
15 M. Bühl, W. Thiel, H. Jiao, P. V. R. Schleyer, M. Saunders and F. A. L. Anet, *J. Am. Chem. Soc.*, 1994, **116**, 6005.
16 (*a*) M. Saunders, H. A. Jiménez-Vázquez, R. J. Cross, S. Mroczkowski, D. I. Freedberg and F. A. L. Anet, *Nature*, 1994, **367**, 256; (*b*) M. Saunders, R. J. Cross, H. A. Jiménez-Vázquez, R. Shimshi and A. Khong, *Science*, 1996, **271**, 1693.
17 M. S. Syamala, R. J. Cross and M. Saunders, *J. Am. Chem. Soc.*, 2002, **124**, 6216.
18 A. Pasquarello, M. Schlüter and R. C. Haddon, *Phys. Rev. A: At., Mol., Opt. Phys.*, 1993, **47**, 1783.
19 K. Yamamoto, M. Saunders, A. Khong, R. J. Cross Jr., M. Grayson, M. L. Gross, A. F. Benedetto and R. B. Weisman, *J. Am. Chem. Soc.*, 1999, **121**, 1591.
20 For the infrared spectrum of $NaPF6{\cdot}H_2O$, A. M. Heyns, *Spectrochim. Acta, Part A*, 1977, **33**, 315.
21 (*a*) T. Ito, T. Hamaguchi, H. Nagino, T. Yamaguchi, J. Washington and C. P. Kubiak, *Science*, 1997, **277**, 660; (*b*) T. Ito, T. Hamaguchi, H. Nagino, T. Yamaguchi, H. Kido, I. S. Zavarine, T. Richmond, J. Washington and C. P. Kubiak, *J. Am. Chem. Soc.*, 1999, **121**, 4625; (*c*) C. H. Londergan and C. P. Kubiak, *Chem.–Eur. J.*, 2003, **9**, 5962.
22 (*a*) F.-W. Grevels, J. Jacke, W. E. Klotzbücher, C. Krüger, K. Seevogel and Y.-H. Tsay, *Angew. Chem., Int. Ed. Engl.*, 1987, **26**, 885; (*b*) J. J. Turner, C. M. Gordon and S. M. Howdle, *J. Phys. Chem.*, 1995, **99**, 17532.
23 M. Pavanello, A. F. Jalbout, B. Trzaskowski and L. Adamowicz, *Chem. Phys. Lett.*, 2007, **442**, 339.
24 (*a*) E. E. B. Campbell, M. Fanti, I. V. Hertel, R. Mitzner and F. Zerbetto, *Chem. Phys. Lett.*, 1998, **288**, 131; (*b*) E. E. B. Campbell, S. Couris, M. Fanti, E. Koudoumas, N. Krawez and F. Zerbetto, *Adv. Mater.*, 1999, **11**, 405; (*c*) J. Zhao, M. Feng, J. Yang and H. Petek, *ACS Nano*, 2009, **3**, 853; (*d*) R. Jorn, J. Zhao, H. Petek and T. Seideman, *ACS Nano*, 2011, **5**, 7858.